Contents lists available at ScienceDirect

Heliyon

journal homepage: www.cell.com/heliyon

Research article

hsa_circ_0101050 regulated by ZC3H13 enhances tumorigenesis in papillary thyroid cancer via m^{6}A modification

Kun Lv , Ping Xie , Qian Yang , Meng Luo , Chan Li *

Department of Tradition Chinese Medicine, Wuhan Third Hospital, Tongren Hospital of Wuhan University, Wuhan 430060, Hubei, China

ABSTRACT

While the regulatory roles of circular RNAs (circRNAs) and zinc finger CCCH-type containing 13 (ZC3H13) were previously reported in various human cancers, the mechanisms underlying their interaction in papillary thyroid cancer (PTC) remain unclear. We aimed to determine the role of hsa_circ_0101050 and its regulatory relationship with ZC3H13 in PTC. The expression levels of hsa_circ_0101050 and ZC3H13 were determined in tumor samples and adjacent normal tissues from 46 patients with PTC and in two PTC cell lines (IHH-4 and PTC-1) using quantitative reverse transcription–polymerase chain reaction. The roles of hsa_circ_0101050 and ZC3H13 in cell viability, wound healing, and migration were determined using knockdown and overexpression approaches in PTC cell lines, and a xenograft model in nude mice was used to determine their role *in vivo*. Methylated RNA immunoprecipitation assay was used to analyze N6-methyladenosine (m^{6}A) modification of hsa_circ_0101050 by ZC3H13. We found hsa_circ_0101050 over-expression and ZC3H13 downregulation in PTC samples and PTC cell lines. In PTC cell lines, silencing hsa_circ_0101050 reduced cell viability and migration whereas its overexpression pro-moted an aggressive PTC phenotype. ZC3H13 increased the m^{6}A modification of hsa_circ_0101050 and repressed its expression. ZC3H13 overexpression inhibited PTC cell viability, migration, and invasion, which were reversed in cells overexpressing hsa_circ_0101050. Taken together, these results suggested that the downregulation of hsa_circ_0101050 mediated by ZC3H13 through m^{6}A modification contributed to its oncogenic effect in PTC development, revealing the ZC3H13–m^{6}A–hsa_circ_0101050 as a potential therapeutic target in PTC.

1. Introduction

Papillary thyroid cancer (PTC) comprises approximately 80 % of all cases of thyroid cancer, which is a common endocrine ma-lignancy exhibiting an increase in incidence in recent years [1,2]. The 5-year survival rate is approximately 95 % in patients with PTC [3]. However, heterogeneous PTC, characterized by diverse molecular, pathologic, and clinical features as well as aggressive muta-tions, has a recurrence rate of up to 25 % [4,5]. Therefore, in-depth elucidation of the underlying molecular mechanisms leading to PTC progression is essential for its early diagnosis and effective treatment.

Circular RNAs (circRNAs), a diverse class of stable, noncoding RNAs with a circular structure, are abundant in mammalian cells [6]. Resistant to exonuclease degradation, circRNAs are key regulators of gene expression networks at transcriptional, epigenetic, and

---

post-transcriptional levels [7,8]. Recent studies have reported the association of several circRNAs with tumorigenic processes in PTC [9]. For example, hsa_circRNA_102002 upregulation in PTC tissues and cells was shown to promote epithelial–mesenchymal transition and cell migration [10] whereas silencing circRAD18 inhibited PTC cell proliferation, metastasis, glucose uptake, and lactate production [11]. One study reported that the upregulation of hsa_circ_0002111 in PTC tissue samples was associated with lymph node metastasis and advanced TNM stage [12]. The role of hsa_circ_0101050, located at chr13:96489339–96519677 and denoted by the gene symbol *UGGT2*, in PTC is unclear.

N6-methyladenosine (m^{6}A) modification of mRNA is a post-transcriptional mechanism that regulates mRNA splicing, nucleation, and translation [13,14]. Reports indicate that m^{6}A modification, mediated by methyltransferases, demethylases, and reader proteins, plays a role in regulating PTC development. For example, six-transmembrane epithelial antigen of the prostate-2 (STEAP2), is stabilized through methyltransferase-like 3 (METTL3)-mediated m^{6}A modification, and its silencing reverses tumor suppression mediated by METTL3 upregulation [15]. In PTC cells, the knockdown of the demethylase fat mass and obesity associated (FTO) enhances the m^{6}A modification of apolipoprotein E (*APOE*), upregulating its expression, thereby inhibiting glycolytic metabolism via the regulation of the interleukin-6 (IL-6)/c-Jun N-terminal kinase 2 (JNK2)/signal transducer and activator of transcription 3 (STAT3) pathway [16]. The reader protein insulin-like growth factor 2 mRNA-binding protein 2 (IGF2BP2) binds to m^{6}A sites in *ERBB2* mRNA and enhances its translation, thereby reducing chemoresistance in chemotherapy-resistant PTC cells [17].

Importantly, m^{6}A modification in PTC cells has been shown to regulate circRNA stability. For example, Ji et al. [18] found that AlkB homolog (ALKBH) increased the m^{6}A modification of circNRIP1, reducing its abundance. Intriguingly, zinc finger CCCH-containing 13 (ZC3H13) is a core m^{6}A methyltransferase, which is overexpressed in cervical cancer and associated with the altered numbers of tumor-infiltrating immune cells [19]. ZC3H13 promotes proliferation in cervical cancer cells by mediating the m^{6}A modification of centromere protein K (*CENPK*) mRNA, thereby promoting DNA replication [20]. Several studies reported the downregulation of ZC3H13 expression in PTC specimens and that ZC3H13 overexpression increased the m^{6}A levels and decreased IQ motif containing GTPase activating protein 1 (*IQGAP1*) mRNA levels [21,22].

In the present study, we aimed to determine whether ZC3H13-mediated m^{6}A modification of hsa_circ_0101050 played a role in PTC. To this end, we determined the expression levels of hsa_circ_0101050 and ZC3H13 in PTC tissue samples from patients and examined the impact of their interaction on tumorigenesis in PTC, with the aim to determine their utility as a novel biomarker for PTC diagnosis.

2. Materials and methods

2.1. Tissue collection

Specimens from PTC and adjacent normal tissues >3 cm from the PTC were collected from 46 patients undergoing surgery at Wuhan Third Hospital. All collected tissues were stored at −80 °C. The present study was approved by the Wuhan Third Hospital Ethics Committee. All patients provided signed informed consent. The characteristics of the patients with PTC are summarized in Table 1.

2.2. Cell culture

Two PTC cell lines, IHH-4 (catalog no. CL-0803) and TPC-1 (catalog no. CL-0643), and normal human primary thyroid follicular

Table 1
Characteristics of papillary thyroid cancer individuals.

Variable	Total = 46	Percentage (%)
Age (mean ± SD)	47.4 ± 10.6	
Sex		
Male	8	17.4
Female	38	82.6
Tumor size (mm, mean ± SD)	8.2 ± 4.9	
Subtype		
Follicular	17	37.0 %
Classic papillary	19	41.3 %
Solid	10	21.7 %
Pathological tumor stage		
T1-T2	21	45.7
T3-T4	25	54.3
Multifocality		
Single	24	52.2
Multiple	22	47.8
Lymphovascular invasion		
Yes	26	56.5
No	20	43.5
Lymph node metastasis		
Yes	23	50.0
No	23	50.0

epithelial (PTFE) cells (catalog no. CL-H023) were obtained from Procell (China). PTC cell lines were cultured in Roswell Park Memorial Institute-1640 medium (Procell) supplemented with 10 % fetal bovine serum (FBS; Procell) at 5 % CO_2 and 37 °C. PTFE cells were cultured in complete PTFE medium (catalog no. CM-H023; Procell). All cell lines were authenticated by short tandem repeat profiling.

2.3. Cell transfection

Small interfering RNA (siRNA) targeting hsa_circ_0101050 (si-circ), scrambled siRNA serving as negative control (si-NC), hsa_circ_0101050 overexpression vector (OE-circ), ZC3H13 overexpression vector (OE-ZC3H13), and empty negative control vector (OE-NC) were purchased from RiboBio (China). Transfection of TPC-1 and IHH-4 cells with siRNAs (50 nM) or overexpression vectors (2 μg/mL) was accomplished using Lipo6000 (Beyotime, China). Forty-eight hours after transfection, gene expression was confirmed by quantitative reverse transcription–polymerase chain reaction (qRT–PCR) prior to subsequent experiments.

2.4. qRT–PCR

Following the manufacturer's protocol, RNA was extracted from cells and tissues using RNAiso Plus (Takara, Japan). The HiScript 1st strand cDNA synthesis kit (Vazyme, China) was used to synthesize cDNA from the extracted RNA. The TB Green fast qPCR mix (Takara) was used to perform qRT–PCR. Data were analyzed using the $2^{-\Delta\Delta Ct}$ method, and glyceraldehyde 3-phosphate dehydrogenase (*GAPDH*) was used for normalization (Supplementary Table 1). Primers used for the amplification of hsa_circ_0101050, *UGGT2*, *ZC3H13*, and *GAPDH* are shown in Table 2.

2.5. RNase R treatment

Cellular RNA was treated with RNase R (Beyotime, China) for 30 min at 37 °C to remove linear RNA. Next, the RNA was amplified to generate cDNA, and the expression levels of hsa_circ_0101050 and its linear transcript (*UGGTA*) were detected using qRT–PCR.

2.6. CCK-8 assay

PTC cell proliferation was assessed using the CCK-8 kit (Beyotime, China). Briefly, 5×10^3 PTC cells were seeded into 96-well plates and 10 μL of the CCK-8 solution was added to the cultures at 0, 24, 48, and 72 h after plating. After an incubation of 90 min, the optical density of the cultures at 450 nm was measured using a microplate reader (Molecular Devices, China).

2.7. Wound-healing assay

Trypsinized IHH-4 and TPC-1 cells (2×10^4) were cultured in 6-well plates until reaching 90 % confluency. Next, a vertical wound was created in wells using a 100-μL pipette tip and the cells were observed at 0 and 24 h under a microscope. The rate of wound closure was determined using the following formula: rate of wound closure = [(wound width at 0 h – wound width at 24 h)/wound width at 0 h] × 100 %.

2.8. Transwell assay

In the transwell assay, 300 μL of medium without FBS containing 2×10^4 IHH-4 or TPC-1 cells was transferred into a Transwell insert precoated with Matrigel. The Transwell insert was then transferred to a new 12-well plate containing 500 μL of medium with 20 % FBS. After 24 h, cells invading the bottom chamber were fixed for 15 min using 4 % paraformaldehyde, stained for 10 min with 0.5 % crystal violet, and imaged using a microscope (Nikon, Japan).

2.9. Methylated RNA immunoprecipitation assay

An anti-m^{6}A antibody (catalog no. ab286164; Abcam, UK) was used for the methylated RNA immunoprecipitation (MeRIP) of the

Table 2
Sequence of primers for qRT-PCR.

Gene	Primer type	Sequence
hsa_circ_0101050	Forward	5′-GTGGTGTGAAACCTGGTGTG-3′
	Reverse	5′-TTGAGTATCTTGCTTTTGAAGCTG-3′
UGGT2	Forward	5′-CTCAAGACTGGCTGTGGTGT-3′
	Reverse	5′-TCCTGTCATGCTTTCGCCTT-3′
ZC3H13	Forward	5′-TCTGATAGCACATCCCGAAGA-3′
	Reverse	5′-CAGCCAGTTACGGCACTGT-3′
GAPDH	Forward	5′- CTGGGCTACACTGAGCACC-3′
	Reverse	5′-AAGTGGTCGTTGAGGGCAATG-3′

m⁶A-modified hsa_circ_0101050. Briefly, 500 μL of MeRIP buffer (catalog no. GS-ET-001; Cloud-seq, China) was added to 100 μg of total RNA extracted from cells using RNAiso Plus (Takara). After incubation with 1 μL of immunoglobulin G (IgG), the IgG was removed using protein A/G beads. The prewashed lysate was transferred to a new tube and incubated with IgG or the m⁶A antibody for 2 h at 4 °C with rotation. Finally, m⁶A-bound RNA was eluted and purified and the enrichment of hsa_circ_0101050 was determined using qRT–PCR.

2.10. Xenograft assay

Twelve male BALB/c nude mice with an approximate weight of 20 g were obtained from Hunan SJA Laboratory Animal (China). The mice were separately housed in standard cages appropriate for their size, with the environment maintained at a relative humidity of 50 % ± 5 % and a temperature of 22 °C ± 2 °C. All mice had unlimited access to sterilized water and rodent chow and were housed under a 12:12-h light–dark cycle. TPC-1 cell lines (1×10^{6}) stably transfected with lentiviral vectors containing OE-NC, OE-ZC3H13, OE-circ, or OE-ZC3H13 plus OE-circ were subcutaneously injected into the mice. During the 35-day feeding period, tumor size was
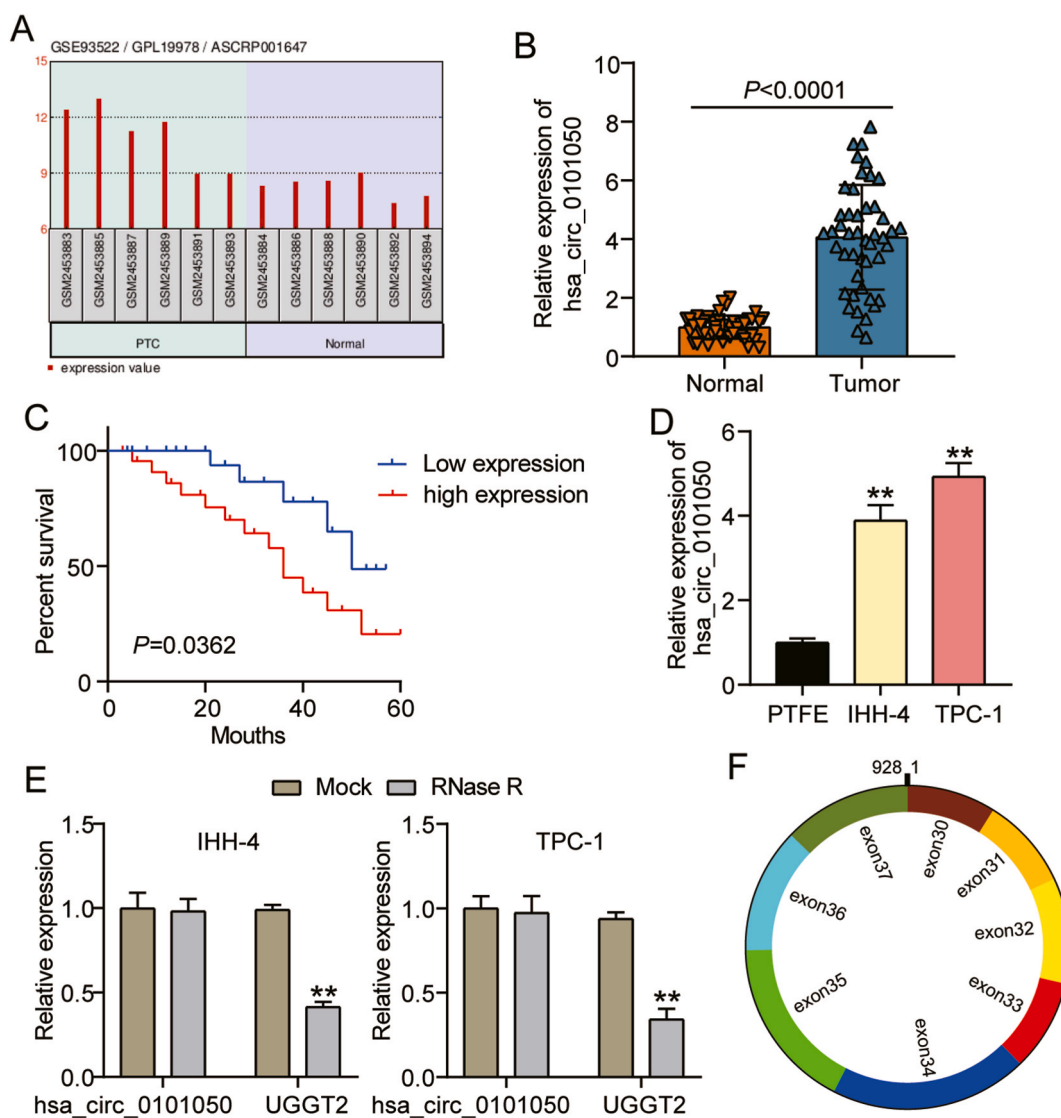
Fig. 1. hsa_circ_0101050 expression is increased in papillary thyroid cancer. A. hsa_circ_0101050 levels in papillary thyroid cancer (PTC) samples based on the analysis of the circRNA microarray dataset GSE93522 from the GEO database. B. Expression levels of hsa_circ_0101050 in patient samples of PTC and the adjacent normal tissue were determined with quantitative reverse transcription–polymerase chain reaction (qRT–PCR). C. Association of hsa_circ_0101050 expression with survival of patients with PTC. D. Expression levels of hsa_circ_0101050 in IHH-4 and TPC-1 cell lines and in normal human primary thyroid follicular epithelial cell (PTFE) were determined using qRT–PCR. **P < 0.001 vs. PTFE. E. Stability of hsa_circ_0101050 was determined with the RNase R assay. **P < 0.001 vs. MOCK. F. Construction of hsa_circ_0101050.

monitored every week using Vernier calipers and tumor volume was calculated using the following formula: tumor volume = 0.5 × tumor length × tumor width^2. At the end of the experiment, all mice were euthanized with CO_2 and the tumors were collected for weighing. The Animal Care and Use Committee of Wuhan Third Hospital approved all animal experiments, which were conducted in strict accordance with the study protocol.
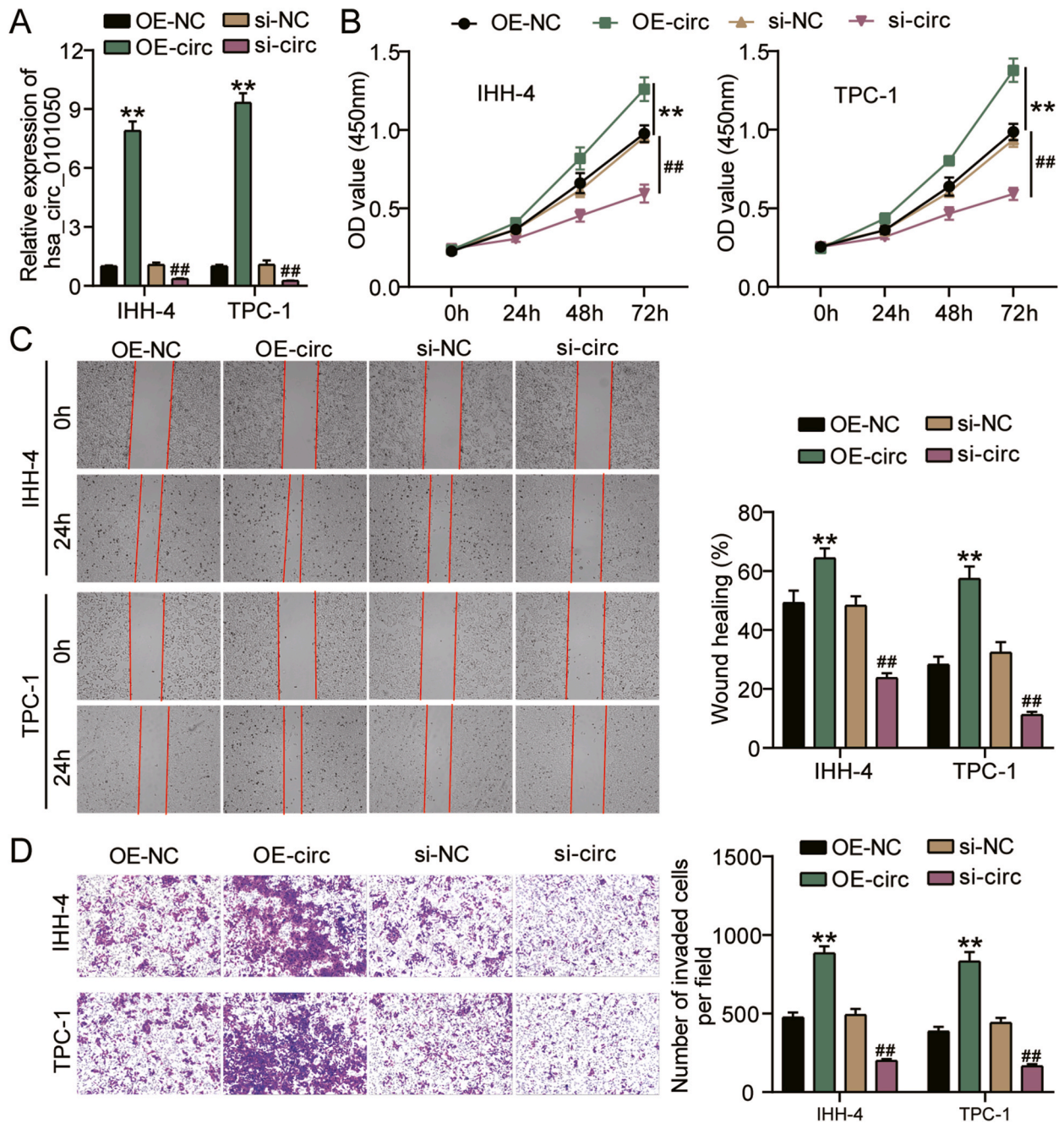
Fig. 2. hsa_circ_0101050 upregulation enhances cell proliferation, migration, and invasion in PTC cells A. Expression levels of hsa_circ_0101050 in IHH-4 and TPC-1 cells transfected with hsa_circ_0101050 siRNA, hsa_circ_0101050 overexpression vector, or the control vector were determined with qRT–PCR. B. Cell proliferation in IHH-4 and TPC-1 cells transfected with hsa_circ_0101050 siRNA, hsa_circ_0101050 overexpression vector, or the control vector were determined using the CCK-8 assay. C. Cell migration ability in IHH-4 and TPC-1 cells transfected with hsa_circ_0101050 siRNA, hsa_circ_0101050 overexpression vector, or the control vector were determined using the wound-healing assay. D. Cell invasion ability in IHH-4 and TPC-10 cells transfected with hsa_circ_0101050 siRNA, hsa_circ_0101050 overexpression vector, or the control vector were revealed using the transwell assay. **P < 0.001 vs. OE-NC; ##P < 0.001 vs. si-NC.

2.11. Hematoxylin–eosin staining

The tumor tissues resected from mice were fixed in 4 % paraformaldehyde, dehydrated with graded ethanol solutions, and embedded in paraffin. The paraffin-embedded tissues were cut into 5-μm-thick sections. After dewaxing and hydration, the sections were stained using the hematoxylin–eosin stain kit (catalog no. G1120; Solarbio, China). Images of the stained specimens were captured using a microscope (Nikon, Japan).

2.12. Statistical analysis

Data (means ± standard deviation) from three biological replicates were analyzed using the GraphPad Prism 8 software. Outcomes from multiple groups were analyzed with one-way analysis of variance. A P value of <0.05 indicated statistically significant differences. The relationship between the expression levels of hsa_circ_0101050 and *ZC3H13* in PTC tissues was evaluated using Pearson's correlation analysis. The relationship between the levels of hsa_circ_0101050 and the prognosis of patients with PTC was evaluated using Kaplan–Meier survival curves.

3. Results

3.1. hsa_circ_0101050 is overexpressed in PTC

According to the circRNA microarray dataset GSE93522 from the GEO database, the hsa_circ_0101050 expression was upregulated in PTC tissue samples (Fig. 1A). Similarly, we found that the hsa_circ_0101050 expression levels were elevated in the PTC tumor samples compared to the adjacent normal tissue samples in the present study cohort (Fig. 1B). The higher expression level of hsa_circ_0101050 was associated with a lower survival rate in patients with PTC (Fig. 1C). A significant increase in hsa_circ_0101050 was observed in the two PTC cell lines that were evaluated (IHH-4 and TPC-1) compared to the control PTFE cells (Fig. 1D). Additionally, RNase R treatment significantly reduced *UGGT2* levels, the gene encoding hsa_circ_0101050, while exhibiting a minimal effect on hsa_circ_0101050 expression (Fig. 1E). The construction of hsa_circ_0101050 was shown in Fig. 1F. Overall, these data suggested that hsa_circ_0101050 was consistently overexpressed in PTC.
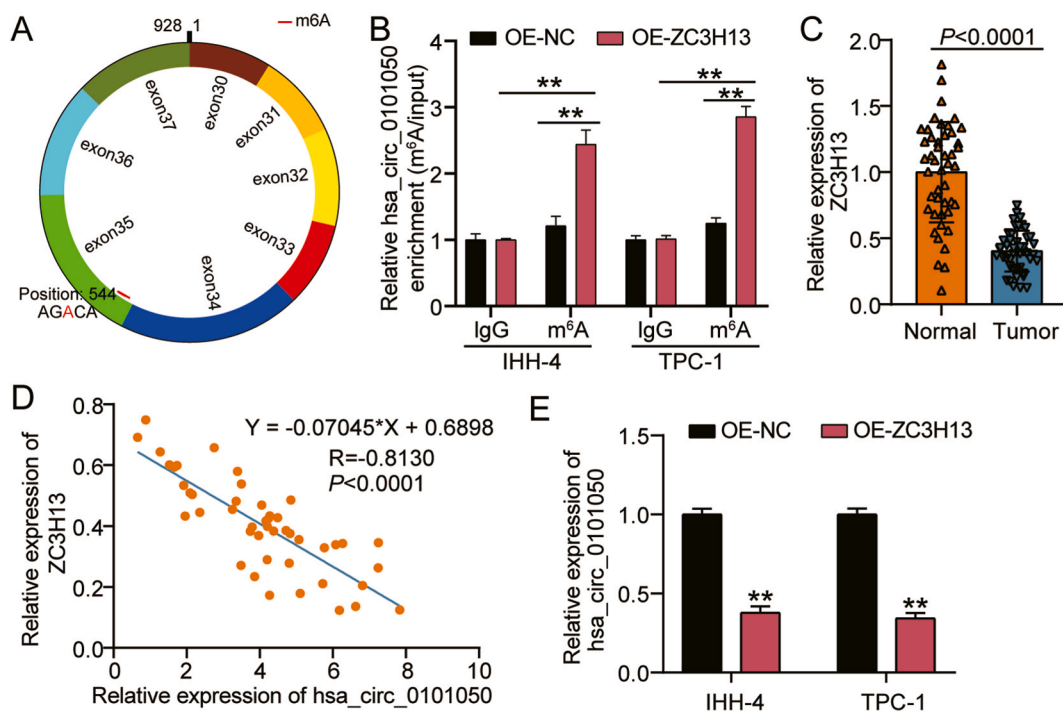
Fig. 3. ZC3H13 was evidenced to mediate m⁶A modification of hsa_circ_0101050. A. CircPrimer2.0 shows the sites of m^{6}A modification in hsa_circ_0101050. B. The levels of m^{6}A modification of hsa_circ_0101050 in IHH-4 and TPC-10 cells transfected with the ZC3H13 overexpression vector were measured with the methylated RNA immunoprecipitation assay. **P < 0.001. C. Expression levels of ZC3H13 in patient samples of PTC and the adjacent normal tissue were determined with qRT–PCR. D. Association of hsa_circ_0101050 and ZC3H13 expression levels in patient samples of PTC was determined with Pearson's correlation analysis. E. Expression levels of hsa_circ_0101050 in IHH-4 and TPC-10 cells overexpressing ZC3H13 or the control vector were determined with qRT–PCR. **P < 0.001 vs. OE-NC.

3.2. hsa_circ_0101050 upregulation enhances PTC cell proliferation, migration, and invasion, while its downregulation inhibits these functions

Next, we investigated the functional implications of the increased hsa_circ_0101050 expression levels in PTC. As shown in Fig. 2A, the hsa_circ_0101050 levels were significantly increased in TPC-1 and IHH-4 cells following OE-circ transfection and notably reduced after si-circ transfection. The CCK-8 assay indicated that the overexpression of hsa_circ_0101050 enhanced the proliferation of IHH-4 and TPC-1 cells, which was reduced in cultures with silenced hsa_circ_0101050 (Fig. 2B). The migratory capacity of IHH-4 and TPC-1 cells was significantly enhanced in cultures overexpressing hsa_circ_0101050 and diminished in those with silenced hsa_circ_0101050, as shown in the wound-healing assay (Fig. 2C). The transwell assay revealed that the overexpression of hsa_circ_0101050 enhanced invasiveness in both IHH-4 and TPC-1 cells, which was suppressed following the silencing of hsa_circ_0101050 (Fig. 2D). These findings clearly demonstrated that hsa_circ_0101050 promoted the development of PTC.
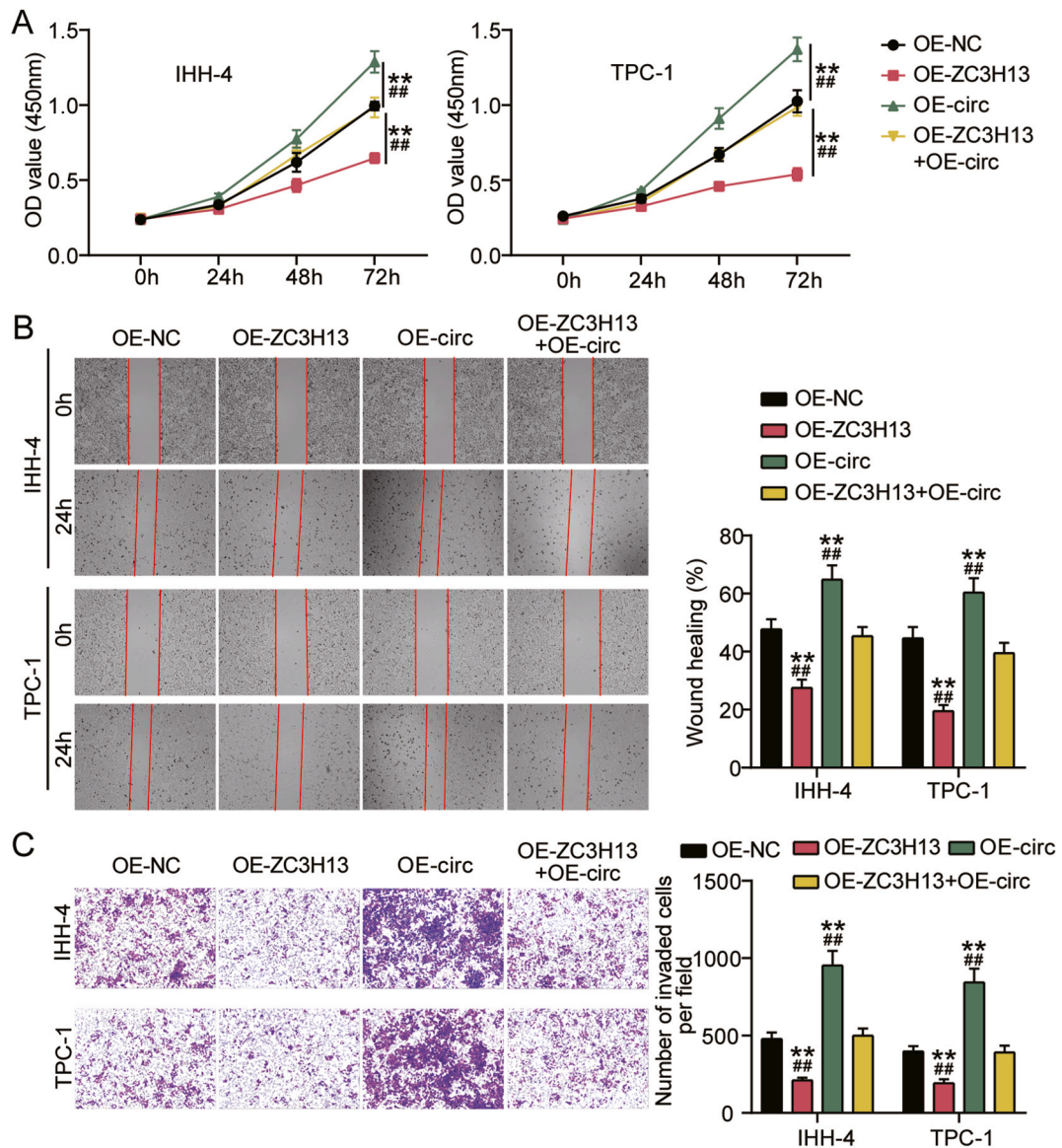
Fig. 4. The inhibitory effect of ZC3H13 on PTC cell malignancy potential is reversed by hsa_circ_0101050 overexpression. A. Proliferation of IHH-4 and TPC-1 cells transfected with the hsa_circ_0101050 or ZC3H13 overexpression vector or the control vector was determined using the CCK-8 assay. B. Cell migration of IHH-4 and TPC-1 cells transfected with the hsa_circ_0101050 or ZC3H13 overexpression vectors or the control vector were determined using the wound-healing assay. C. Cell invasion of IHH-4 and TPC-10 cells transfected with the hsa_circ_0101050 or ZC3H13 overexpression vectors or the control vector were determined using the transwell assay. **P < 0.001 vs. OE-NC. ##P < 0.001 vs. OE-ZC3H13+OE-circ.

3.3. ZC3H13 mediates the m⁶A modification of hsa_circ_0101050

CircPrimer 2.0, a widely used circRNA analysis tool, revealed the m^6A modification sites of hsa_circ_0101050, as illustrated in Fig. 3A. The MeRIP assay indicated that the overexpression of ZC3H13 significantly increased the m^6A modification of hsa_-circ_0101050 in both IHH-4 and TPC-1 cells (Fig. 3B). The assessment of *ZC3H13* levels using qRT–PCR confirmed the downregulation of ZC3H13 expression in PTC tissue samples of the study patients (Fig. 3C). Additionally, hsa_circ_0101050 and *ZC3H13* expression levels were negatively correlated in these PTC tissue samples (Fig. 3D). Furthermore, the expression levels of hsa_circ_0101050 were significantly lower in TPC-1 and IHH-4 cells overexpressing ZC3H13 (Fig. 3E), suggesting that ZC3H13 upregulated the m^6A modification of hsa_circ_0101050 and suppressed its mRNA expression.

3.4. The inhibitory effect of ZC3H13 on PTC cell malignancy is reversed by hsa_circ_0101050 overexpression

Next, we performed rescue experiments to elucidate the interaction between ZC3H13 and hsa_circ_0101050 during PTC development. Functionally, ZC3H13 overexpression reduced the proliferative ability of IHH-4 and TPC-1 cells, which was partially reversed with hsa_circ_0101050 overexpression (Fig. 4A). Similarly, ZC3H13 overexpression attenuated the migration and invasion capabilities of IHH-4 and TPC-1 cells, which were significantly reversed in cells overexpressing hsa_circ_0101050 (Fig. 4B and C). Overall, these results indicated that ZC3H13 suppressed PTC malignancy, thereby counteracting the oncogenic effects of hsa_circ_0101050.

3.5. ZC3H13 inhibits PTC cell growth by depleting hsa_circ_0101050 in vivo

In addition to their function in cells *in vitro*, we used an animal model to investigate the roles of ZC3H13 and hsa_circ_0101050 in solid tumor growth. In our model, the tumor volume and size were reduced in mice injected with PTC cells stably transfected with OE-
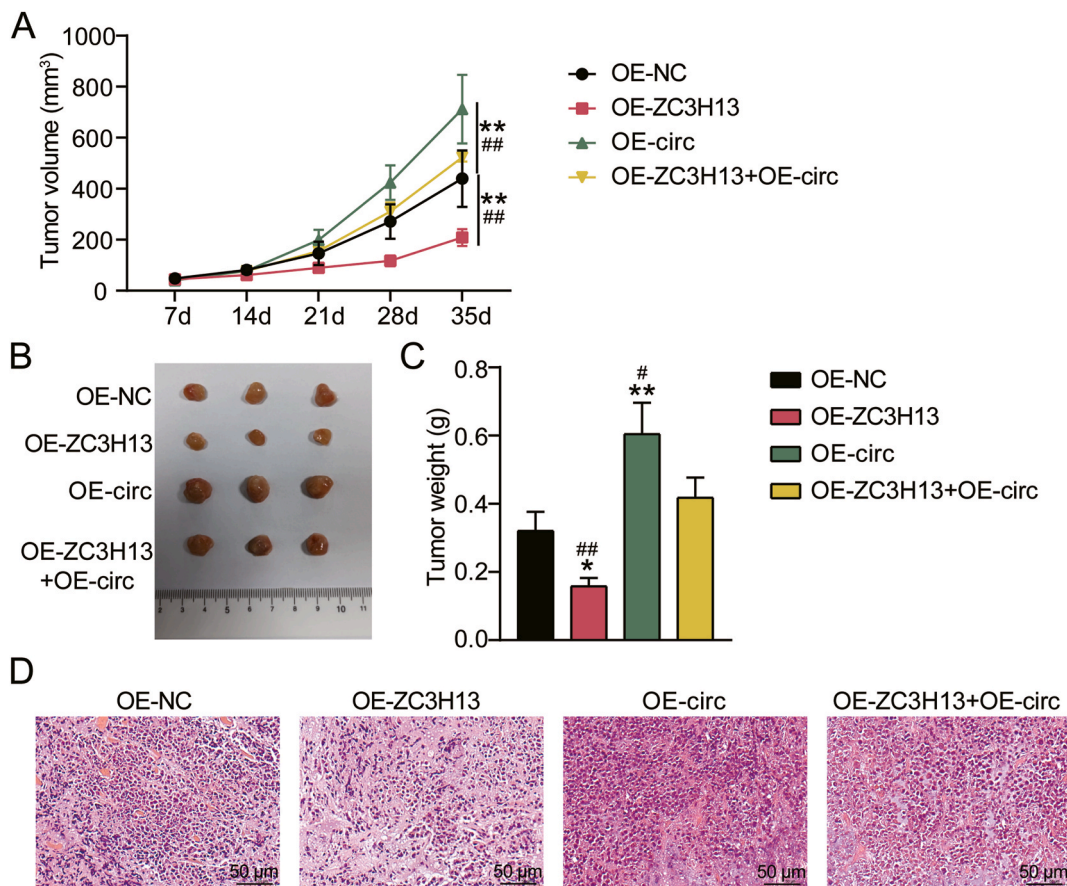
Fig. 5. ZC3H13 inhibits PTC cell growth by depleting hsa_circ_0101050 *in vivo*. A–C. To create the xenograft model of PTC, TPC-1 cells stably transfected with the hsa_circ_0101050 or the ZC3H13 overexpression vector or the control vector were injected into nude mice and tumor volume (A), size (B), and weight (C) were evaluated once a week during the 35-day period to assess tumor progression. *$P < 0.05$, **$P < 0.001$ vs. OE-NC; #$P < 0.05$, ##$P < 0.001$ vs. OE-ZC3H13+OE-circ. (D) Representative images of hematoxylin–eosin-stained tumor tissues from mice in different groups are shown.

ZC3H13 (Fig. 5A and B). Moreover, the tumor volume and size were larger in mice injected with PTC cells stably transfected with OE-circ, and hsa_circ_0101050 overexpression reversed the tumor-suppressive effect of ZC3H13 (Fig. 5A and B). The overexpression of ZC3H13 significantly reduced tumor growth, which was promoted by hsa_circ_0101050 overexpression, indicating the reversal of the effects of ZC3H13 by hsa_circ_0101050 (Fig. 5C). The hematoxylin–eosin staining revealed that the tumor cells in the OE-NC group were closely arranged with a complete structure and that the tumor cells in the OE-ZC3H13 group were loosely arranged with incomplete cell membranes, pyknotic or cracking nuclei, and cavity-shaped organization. Additionally, the tumor cells in the OE-circ group were more closely arranged than those in the OE-NC group and the tumor cells in the OE-ZC3H13+OE-circ group were similar to those in the OE-NC group (Fig. 5D). Overall, these results indicated that the inhibition of PTC cell growth by ZC3H13 was relieved by hsa_circ_0101050.

4. Discussion

In the present study, we used complementary *in vitro* and *in vivo* approaches to show that hsa_circ_0101050 was significantly overexpressed in PTC tissue sections and that its upregulation promoted invasion, migration, and proliferation of PTC cells *in vitro*, while accelerating tumor growth *in vivo*. Conversely, inhibiting hsa_circ_0101050 significantly reduced the malignancy potential of PTC cells. Upregulation of ZC3H13 counteracted the tumor-promoting effects of hsa_circ_0101050 overexpression by mediating its m^6A modification. These results suggest that targeting the m^6A modification of hsa_circ_0101050 by ZC3H13 should be considered a novel therapeutic approach in PTC.

Increasing evidence suggests that circRNAs contribute to tumorigenesis by controlling gene regulation at various levels [23]. Numerous circRNAs have been shown to be involved in the tumorigenesis of PTC [24]. For example, circ_0015278 is suppressed in PTC whereas higher circ_0015278 levels are associated with the lack of extrathyroidal infiltration and lower recurrence rates [25]. Furthermore, circ_0011385 promotes the persistent invasion and proliferation of PTC cells by stabilizing cyclin D1 mRNA and enhancing its protein synthesis, thereby contributing to PTC development [26]. Silencing circ_PRKCI suppresses glucose uptake and lactate production, halts cell cycle progression, and promotes cancer remission in PTC [27]. This is the first study to demonstrate the elevated expression of the newly identified hsa_circ_0101050 in PTC. Our analyses reveal that hsa_circ_0101050 exhibits a positive role in controlling the proliferation, invasiveness, and migratory capacity of tumor cells, thereby promoting PTC progression. Similar roles have been ascribed to other circRNAs in previous studies. For example, circ_0067934 has been reported to promote PTC progression by enhancing PTC cellular proliferation, invasiveness, and migratory capacity [28]. Similarly, circ_0003747 has been demonstrated to promote PTC cell proliferation, invasion, and metastasis, thereby accelerating PTC tumorigenesis [29].

Various cytoplasmic circRNAs have been shown to contribute to tumor progression by undergoing m^6A modification. In liver cancer, upregulation of hsa_circ_0095868 is associated with m^6A modification and reduced patient survival [30]. METTL3, the host gene of circMETTL3, stabilizes circMETTL3 expression in an m^6A-dependent manner and promotes malignancy in breast cancer cells [31]. The METTL3-mediated m^6A modification of circQSOX1 RNA, recognized by IGF2BP2, enhances glycolysis and facilitates immune evasion in colorectal cancer cells [32]. Furthermore, in PTC, ALKBH5 significantly enhances the m^6A modification of circNRIP1, inhibiting its expression and subsequently suppressing glycolysis and tumorigenesis [18]. Our analyses indicate that the hsa_circ_0101050 sequence includes an m^6A modification site, suggesting that hsa_circ_0101050 role in promoting PTC could be due to m^6A modification.

ZC3H13 has been recently recognized as an m^6A regulator based on its ability to bind m^6A-modified RNAs and enhance their stability [33]. Studies have demonstrated that the m^6A modification of IQGAP1 mRNA is increased in PTC cells overexpressing ZC3H13 [22]. Our findings confirm that ZC3H13 is also involved in the m^6A modification of PTC cells, consistent with previous results. Additionally, ZC3H13 has been reported to bind to circRNAs. For example, ZC3H13 is recruited by hsa_circ_0000848 to stabilize SMAD7 expression, thereby regulating apoptosis in cardiomyocytes [34]. In PTC, we found that ZC3H13 inhibited hsa_circ_0101050 expression by binding and regulating its m^6A modification, thereby inhibiting its expression, which is a novel finding. Furthermore, our finding that ZC3H13 overexpression counteracts the negative impact of hsa_circ_0101050 on PTC cells suggests that hsa_circ_0101050 can promote PTC development through ZC3H13-mediated m^6A modification.

Our findings confirm that hsa_circ_0101050 plays a role in PTC development and reveals the underlying mechanism. However, the limitations of our study should also be acknowledged. We did not elucidate the signaling pathways downstream from hsa_circ_0101050. A previous study indicated that ZC3H13 played a role in tumorigenesis by inhibiting the RAS–ERK signaling pathway [35]. Therefore, future studies should investigate the signaling pathways downstream from ZC3H13-mediated m^6A modification of hsa_circ_0101050. In the present study, we used only one siRNA targeting hsa_circ_0101050 and did not evaluate the potential off-target effects of our approach. Our findings should be confirmed in future studies utilizing additional siRNAs. Additionally, we did not evaluate the role of this pathway in resistance to treatment, such as radioiodine, in PTC cells [36]. Future studies will explore the association of hsa_circ_0101050 with radioiodine resistance in PTC.

5. Conclusion

Our complementary *in vitro* and *in vivo* studies reveal that the newly identified hsa_circ_0101050 promotes invasion, migration, and proliferation of PTC through its m^6A modification mediated by ZC3H13, providing a novel target for the development of effective treatment strategies for PTC.

Data availability statement

Data will be made available on request.

Ethics declarations

Funding

CRediT authorship contribution statement

Kun Lv: Writing – original draft, Validation, Methodology, Conceptualization. **Ping Xie:** Visualization, Formal analysis, Data curation. **Qian Yang:** Formal analysis, Data curation. **Meng Luo:** Formal analysis, Data curation. **Chan Li:** Writing – review & editing, Writing – original draft, Funding acquisition.

Declaration of competing interest

The authors declare that they have no known competing financial interests or personal relationships that could have appeared to influence the work reported in this paper.

Acknowledgements

Appendix A. Supplementary data

Supplementary data to this article can be found online at https://doi.org/10.1016/j.heliyon.2024.e32913.

References

[1] L.P.A. Arboleda, et al., Global frequency and distribution of head and neck cancer in pediatrics, a systematic review, Crit. Rev. Oncol. Hematol. 148 (2020) 102892.

[2] J. Lou, et al., Analysis of the influence factors of cervical lymph node metastasis in Papillary thyroid carcinoma: a retrospective observational study, Medicine (Baltim.) 102 (36) (2023) e35045.

[3] J.W. Seo, et al., Application of metabolomics in prediction of lymph node metastasis in papillary thyroid carcinoma, PLoS One 13 (3) (2018) e0193883.

[4] W. Dong, et al., Time-varying pattern of mortality and recurrence from papillary thyroid cancer: lessons from a long-term follow-up, Thyroid 29 (6) (2019) 802–808.

[5] K. Kim, et al., The updated AJCC/TNM staging system for papillary thyroid cancer (8th edition): from the perspective of genomic analysis, World J. Surg. 42 (11) (2018) 3624–3631.

[6] J. Dong, et al., Challenges and opportunities for circRNA identification and delivery, Crit. Rev. Biochem. Mol. Biol. 58 (1) (2023) 19–35.

[7] I.L. Patop, S. Wust, S. Kadener, Past, present, and future of circRNAs, EMBO J. 38 (16) (2019) e100836.

[8] L.S. Kristensen, et al., The emerging roles of circRNAs in cancer and oncology, Nat. Rev. Clin. Oncol. 19 (3) (2022) 188–206.

[9] G. Zhu, et al., CircRNA: a novel potential strategy to treat thyroid cancer, Int. J. Mol. Med. 48 (5) (2021) (Review).

[10] W. Zhang, et al., Hsa_circRNA_102002 facilitates metastasis of papillary thyroid cancer through regulating miR-488-3p/HAS2 axis, Cancer Gene Ther. 28 (3–4) (2021) 279–293.

[11] W. Chen, et al., Upregulated circRAD18 promotes tumor progression by reprogramming glucose metabolism in papillary thyroid cancer, Gland Surg. 10 (8) (2021) 2500–2510.

[12] G. Du, et al., Increased expression of hsa_circ_0002111 and its clinical significance in papillary thyroid cancer, Front. Oncol. 11 (2021) 644011.

[13] R. Kumari, et al., mRNA modifications in cardiovascular biology and disease: with a focus on m6A modification, Cardiovasc. Res. 118 (7) (2022) 1680–1692.

[14] I.A. Roundtree, et al., Dynamic RNA modifications in gene expression regulation, Cell 169 (7) (2017) 1187–1200.

[15] Y. Zhu, et al., METTL3-mediated m6A modification of STEAP2 mRNA inhibits papillary thyroid cancer progress by blocking the Hedgehog signaling pathway and epithelial-to-mesenchymal transition, Cell Death Dis. 13 (4) (2022) 358.

[16] J. Huang, et al., FTO suppresses glycolysis and growth of papillary thyroid cancer via decreasing stability of APOE mRNA in an N6-methyladenosine-dependent manner, J. Exp. Clin. Cancer Res. 41 (1) (2022) 42.

[17] R. Sa, et al., IGF2BP2-dependent activation of ERBB2 signaling contributes to acquired resistance to tyrosine kinase inhibitor in differentiation therapy of radioiodine-refractory papillary thyroid cancer, Cancer Lett. 527 (2022) 10–23.

[18] X. Ji, et al., ALKBH5-induced circular RNA NRIP1 promotes glycolysis in thyroid cancer cells by targeting PKM2, Cancer Sci. 114 (6) (2023) 2318–2334.

[19] H. Ji, et al., Comprehensive characterization of tumor microenvironment and m6A RNA methylation regulators and its effects on PD-L1 and immune infiltrates in cervical cancer, Front. Immunol. 13 (2022) 976107.

[20] X. Lin, et al., N(6)-methyladenosine modification of CENPK mRNA by ZC3H13 promotes cervical cancer stemness and chemoresistance, Mil Med Res 9 (1) (2022) 19.

[21] J. Hou, et al., m(6)A RNA methylation regulators have prognostic value in papillary thyroid carcinoma, Am. J. Otolaryngol. 41 (4) (2020) 102547.

[22] R. Xie, et al., Overexpressed ZC3H13 suppresses papillary thyroid carcinoma growth through m6A modification-mediated IQGAP1 degradation, J. Formos. Med. Assoc. 122 (8) (2023) 738–746.

[23] L. Chen, G. Shan, CircRNA in cancer: fundamental mechanism and clinical potential, Cancer Lett. 505 (2021) 49–57.

[24] H. Ye, et al., The emerging roles of circRNAs in papillary thyroid carcinoma: molecular mechanisms and biomarker potential, Protein Pept. Lett. 30 (9) (2023) 709–718.

[25] H. Ding, et al., Higher circular RNA_0015278 correlates with absence of extrathyroidal invasion, lower pathological tumor stages, and prolonged disease-free survival in papillary thyroid carcinoma patients, J. Clin. Lab. Anal. 35 (7) (2021) e23819.

[26] X. Yao, et al., Circular RNA EIF3I promotes papillary thyroid cancer progression by interacting with AUF1 to increase Cyclin D1 production, Oncogene (2023).

[27] Y. Liu, et al., Silencing circRNA protein kinase C iota (circ-PRKCI) suppresses cell progression and glycolysis of human papillary thyroid cancer through circ-PRKCI/miR-335/E2F3 ceRNA axis, Endocr. J. 68 (6) (2021) 713–727.

[28] L.P. Dong, et al., circ_0067934 promotes the progression of papillary thyroid carcinoma cells through miR-1301-3p/HMGB1 axis, Neoplasma 69 (1) (2022) 1–15.

[29] Y. Yao, et al., Hsa_circ_0058124 promotes papillary thyroid cancer tumorigenesis and invasiveness through the NOTCH3/GATAD2A axis, J. Exp. Clin. Cancer Res. 38 (1) (2019) 318.

[30] A. Du, et al., M6A-mediated upregulation of circMDK promotes tumorigenesis and acts as a nanotherapeutic target in hepatocellular carcinoma, Mol. Cancer 21 (1) (2022) 109.

[31] Z. Li, et al., CircMETTL3, upregulated in a m6A-dependent manner, promotes breast cancer progression, Int. J. Biol. Sci. 17 (5) (2021) 1178–1190.

[32] Z. Liu, et al., N6-methyladenosine-modified circular RNA QSOX1 promotes colorectal cancer resistance to anti-CTLA-4 therapy through induction of intratumoral regulatory T cells, Drug Resist. Updates 65 (2022) 100886.

[33] Z. Cai, et al., ELAVL1 promotes prostate cancer progression by interacting with other m6A regulators, Front. Oncol. 12 (2022) 939784.

[34] S. Cao, et al., Circular RNA hsa_circ_0000848 regulates cardiomyocyte proliferation and apoptosis under hypoxia via recruiting ELAVL1 and stabilizing SMAD7 mRNA, Anatol. J. Cardiol. 26 (3) (2022) 189–197.

[35] D. Zhu, et al., ZC3H13 suppresses colorectal cancer proliferation and invasion via inactivating Ras-ERK signaling, J. Cell. Physiol. 234 (6) (2019) 8899–8907.

[36] L. Shi, et al., LncRNA GLTC targets LDHA for succinylation and enzymatic activity to promote progression and radioiodine resistance in papillary thyroid cancer, Cell Death Differ. 30 (6) (2023) 1517–1532.